Opioid-induced neuroanatomical, microglial and behavioral changes are blocked by suvorexant without diminishing opioid analgesia

Ronald McGregor[1,2,3], Ming-Fung Wu [1,2,3], Thomas C. Thannickal[1,2], Songlin Li[1,2] & Jerome M. Siegel [1,2] ✉

Heroin use disorder in humans and chronic opioid administration to mice result in an increase in the number and a decrease in the size of detected hypocretin (Hcrt, or orexin) neurons. Chronic morphine administration to mice increases Hcrt axonal projections to the ventral tegmental area (VTA), the level of tyrosine hydroxylase (TH) in VTA and the number of detected TH⁺ cells in VTA, and activates VTA and hypothalamic microglia. Co-administration of morphine with the dual Hcrt receptor antagonist suvorexant prevents morphine-induced changes in the number and size of Hcrt neurons, the increase in Hcrt projections to the VTA and microglial activation in the VTA and hypothalamus. Co-administration of suvorexant with morphine also prevents morphine anticipatory behavior and reduces opioid withdrawal symptoms. However, suvorexant does not diminish morphine analgesia. Here we show that combined administration of opioids and suvorexant may reduce the addiction potential of opioid use for pain relief in humans while maintaining the analgesic effects of opioids.

The annual US rate of opioid overdose deaths now exceeds 76,000, much greater than the annual rates of automobile or gun deaths (Centers for Disease Control and Prevention; https://www.cdc.gov/index.html). Of those who began abusing opioids in the 2000s, 75% reported that their first opioid was prescribed for the relief of pain[1,2]. This progressed to illegal opioid pill acquisition or to heroin or fentanyl use[3,4]. Nonopioid analgesics can be used for relatively minor pain; however, severe burns, cancer, joint inflammation, sickle cell disease, bone damage and many other painful conditions often cannot be effectively treated with nonopioid analgesics. These disorders cause immense suffering.

In our studies of human narcolepsy, which we found to be caused by a loss of hypocretin (Hcrt) neurons[5], as was then reported in greater detail[6,7], we encountered a 'control' human brain with a 54% higher number of detected Hcrt neurons than in any other control. Further investigation led to the discovery that this individual suffered from heroin use disorder (HUD). We then analyzed brains of humans with HUD and found that all have increased numbers of detected Hcrt neurons and that Hcrt neurons were significantly smaller than in human controls. We determined that daily morphine injection in mice for 14 or more days produced an increase in the number of detected Hcrt neurons and a marked shrinkage of these neurons, as in humans with HUD[8]. Cocaine or fentanyl were then found to produce similar changes in Hcrt cell numbers in rats[9,10]. It has long been noted that human narcoleptics, who have an average 90% loss of Hcrt neurons and very low cerebrospinal fluid levels of Hcrt, show little if any evidence of drug abuse, dose escalation or overdose[11], despite their daily prescribed use of gamma hydroxybutyrate, methylphenidate and amphetamine. These drugs, which reverse the sleepiness and cataplexy of narcolepsy, are frequently abused in
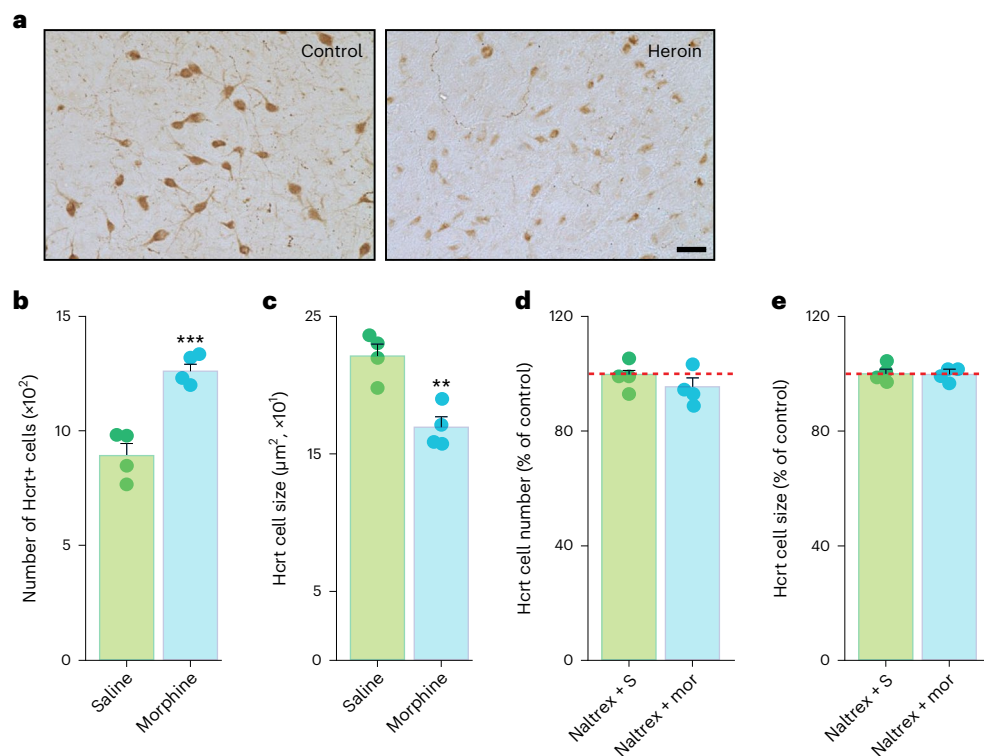
Fig. 1 | Involvement of opioid receptors in the increased number of detected Hcrt neurons and the shrinkage in Hcrt neuron size caused by opioids.
a–**c**, Humans with HUD (human control, male 61 years old and human with HUD, male 71 years old (**a**)) and mice given 50 mg kg⁻¹ of morphine for 14 days showed an increase in the number ($t = 9.793$, d.f. 6, $P < 0.001$, t-test, $n = 4$ per condition (**b**)) and a decrease in the size ($t = 4.315$, d.f. 6, $P = 0.005$, t-test, $n = 4$ per condition (**c**)) of Hcrt-producing neurons. **d**,**e**, These anatomical effects induced by

morphine were blocked in mice by the concurrent administration of the opioid receptor blocker naltrexone (cell number, $t = 0.805$, d.f. 6, $P = 0.452$, t-test, $n = 4$ per condition (**d**)) and cell size, $t = 0.115$, d.f. 6, $P = 0.912$, t-test, $n = 4$ per condition (**e**)). S, saline; mor, morphine. All data presented as mean ± s.e.m. and all tests are two tailed. **$P < 0.01$ and ***$P < 0.001$ (comparing saline versus morphine conditions). Scale bar, 50 μm.

the general population with considerable loss of life[12,13]. Human narcoleptics have a greatly reduced reward activation of the ventral tegmental area (VTA), amygdala and nucleus accumbens (NAc)[14] and altered processing of humor in the hypothalamus and amygdala[15].

We[16–20] and others[10] have demonstrated that increased neuronal discharge in Hcrt neurons is linked to the performance of rewarded tasks in wild-type (WT) mice, rats and dogs. Mice in which the Hcrt peptide is genetically knocked out (Hcrt–KOs) learn a bar press task for food or water as quickly as their WT littermates. However, when the effort to obtain the reward is increased in a 'progressive ratio', they all quit the task within 1 h, whereas their WT littermates continue bar pressing until the end of the 2 h test period. In contrast, the Hcrt–KOs perform as well as WT controls on progressive ratio avoidance tasks, suggesting an emotional specificity in their response deficit[17]. Normal dogs playing in a yard have a large increase in cerebrospinal Hcrt levels. But when these same dogs are induced to run on a treadmill, there is no change in Hcrt level, despite similar elevations in heart rate, respiratory rate and blood pressure[20]. We further found that Hcrt is released in the brain of humans when they are engaged in tasks they enjoy, but not when they are aroused by pain or when they are feeling sad[21].

Dopamine (DA) neurons, particularly those located in the VTA, are known to play a significant role in opioid use disorder (OUD)[22,23]. Hcrt and DA are evolutionarily linked from both a neurochemical and anatomical perspective[24]. VTA plasticity associated with drug rewards requires functional Hcrt receptors[25]. The levels of DA and its major metabolites in the NAc are markedly increased by the microinjection of Hcrt into the VTA[26,27]. Hcrt axons project to the VTA but do not frequently make direct synaptic contact with DA neurons in the VTA, suggesting a volume transmission mechanism[28].

Most studies of the central nervous system effects of opioids have been focused on neurons. However, microglia, resident immune cells of the central nervous system with important roles in brain homeostasis and synaptic function[29–31], have been found to play a role in OUD[32,33]. Chronic opioid exposure results in activated microglia in supraspinal regions, including the NAc and VTA[34]. Blocking microglial activation reduces morphine-induced reward behavior[35]. Microglia express receptors for opioids[36] and HcrtR1 (ref. 37) indicating that these cells can be directly affected by opioids and by Hcrt.

Owing to the role of Hcrt neurons in reward in rodents and pleasure in humans[17,21], we wanted to test the hypothesis that blocking Hcrt receptors might affect brain systems that mediate OUD. In this Article, we found that blockade of Hcrt receptors with the dual Hcrt receptor antagonist suvorexant prevented opioid-induced changes in the size and number of Hcrt neurons and increases in Hcrt projections to the VTA. Suvorexant also prevented opioid-induced microglial activation. In addition, suvorexant prevented morphine anticipatory wheel running activity and significantly reduced opioid withdrawal symptoms. However, blocking Hcrt receptors with suvorexant did not diminish the analgesia produced by opioids. These data suggest that combined administration of Hcrt receptor blockers with opioids can allow potent opioid analgesia, while reducing the risk of developing the anatomical and behavioral changes associated with chronic opioid administration.

Results

Opioid receptors and Hcrt anatomical changes
Our prior work in humans with HUD (Fig. 1a) and in mice given subcutaneous (SC) injections of morphine (50 mg kg⁻¹) for 14 or more days[8] (Fig. 1b,c) showed that opioids increase the number of detected
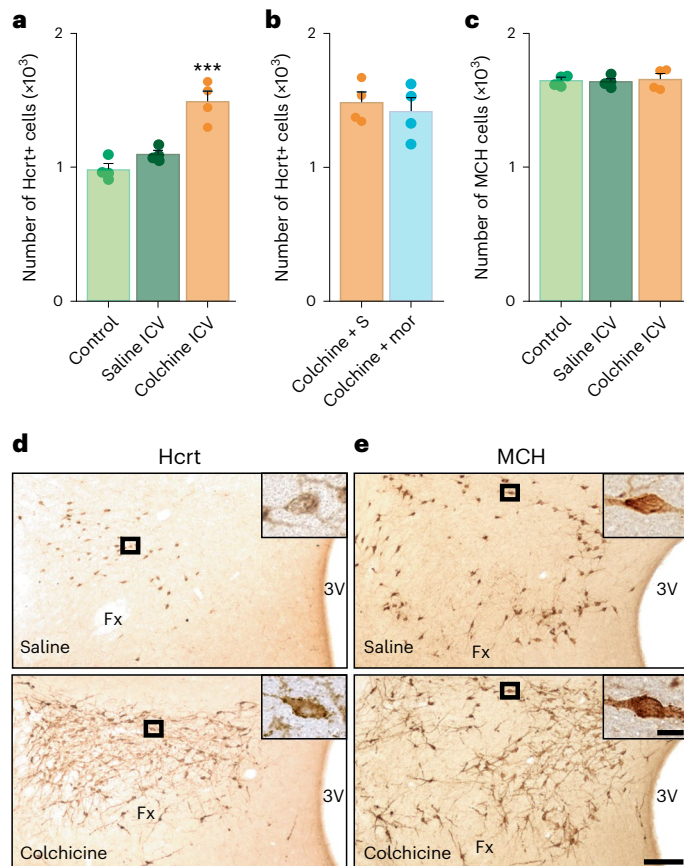
Fig. 2 | Chronic opioid administration does not induce Hcrt expression in non-Hcrt neurons. a, ICV administration of the microtubule transport blocker colchicine (in otherwise drug-free mice) increased the number of 'detected' Hcrt cells in mice by 44%. The increase in cell number after colchicine was significant (all $P < 0.001$, Tukey post hoc compared with control and saline ICV conditions, $n = 4$ per condition). **b**, Hcrt cell number was not further increased by chronic morphine administration in colchicine treated animals ($t = 0.537$, d.f. 6, $P = 0.611$, t-test, $n = 4$ per condition). **b–e**, Colchicine increased the number of Hcrt neurons, but did not significantly alter the number of MCH neurons ($F = 0.108$; d.f. 2, 9; $P = 0.898$, ANOVA, $n = 4$ per condition). All data presented as mean ± s.e.m. and all tests are two tailed. ***$P < 0.001$, compared with control and saline ICV conditions. Representative examples of immunohistochemically labeled Hcrt (**d**) and MCH (**e**) neurons in saline ICV (top) and colchicine ICV (bottom) conditions. Insets are higher (×40) magnification photomicrographs of the selected area (black square) for each condition illustrating individual neurons from animals treated with saline or with colchicine. Note the increases in the intracellular staining of both Hcrt and MCH neurons after colchicine. Scale bar, 100 μm; inset 10 μm. Fx, fornix; 3V, third ventricle.

Hcrt-producing neurons (Fig. 1b, $t = 9.793$, d.f. 6, $P < 0.001$, t-test), and decrease the size of Hcrt neurons (Fig. 1c, $t = 4.315$, d.f. 6, $P = 0.005$, t-test). In Fig. 1d,e we show, in a control for opioid receptor involvement in opioid-induced changes, that these effects are blocked in mice that were given the opioid receptor antagonist naltrexone (50 mg kg^{-1}, SC) 30 min before each daily 50 mg kg^{-1} morphine dose for 14 days. When naltrexone was given before morphine there were no significant changes in Hcrt cell number (Fig. 1d, $t = 0.805$, d.f. 6, $P = 0.452$) or size (Fig. 1e, $t = 0.115$, d.f. 6, $P = 0.912$). This shows, as one might expect, that the morphine effects on Hcrt neurons number and size are mediated by opioid receptors. However, naltrexone not only prevents opioid-induced changes in Hcrt neuron number and size, it also eliminates opioid analgesia[38].

Opioid administration and Hcrt expression

We have previously shown that morphine administration does not cause neurogenesis, based on BrdU and doublecortin studies[8]. However,

Spitzer has reported 'neuronal neurotransmitter respecification' in neurons, that is, that existing neurons could under certain conditions acquire a 'new' transmitter[39]. Therefore, we could not rule out the possibility that chronic morphine administration was inducing the expression of Hcrt peptides in neurons that would not otherwise express these peptides. To examine this possibility, we used colchicine, an inhibitor of microtubule polymerization and thus of axonal transport, to increase the concentration of neurotransmitters in neuronal somas[40]. If neurotransmitter respecification occurred after morphine administration, co-administration of colchicine and morphine should result in detection of a greater number of Hcrt neurons compared with administration of colchicine or morphine alone, since this condition would reveal Hcrt neurons that constitutively express the peptides plus the 'new' neurons recruited to synthesize Hcrt as a result of exposure to morphine.

We found that intracerebroventricular (ICV) injection of colchicine in naive mice increased the number of detected Hcrt neurons by 44% (Fig. 2a, all $P < 0.001$, Tukey post hoc, compared with control and saline ICV conditions). This is comparable to the percent increase in the number of Hcrt neurons seen in mice after morphine (50 mg kg^{-1} for 14 days; Fig. 1b and ref. 8). Figure 2b shows that colchicine together with morphine did not further increase the number of cells labeled relative to colchicine plus saline ($t = 0.537$, d.f. 6, $P = 0.611$, t-test). Together, Fig. 2a,b shows that there is a ceiling to morphine effects on Hcrt neuronal number, implying that there is a fixed number of neurons capable of producing Hcrt, with 44% beyond the baseline number of these cells detected in mice and as much as 54% beyond the baseline number in humans with HUD[8]. This is compatible with our conclusion that the morphine-induced increase in the number of detected Hcrt neurons is not due to neurogenesis or transmitter respecification, but rather to increased Hcrt peptide production leading to the detection of more of the neurons capable of producing Hcrt[8]. Figure 2c shows that colchicine did not have any effect on the number of melanin concentrating hormone (MCH) expressing neurons ($F = 0.108$; d.f. 2, 9; $P = 0.898$, analysis of variance (ANOVA)), even though the intensity of intracellular staining of both Hcrt and MCH neuronal populations are similarly increased by the presence of colchicine. This is illustrated in Fig. 2d for Hcrt, and Fig. 2e for MCH (top saline, bottom colchicine). MCH is a peptide of similar size to Hcrt, and the anatomical distribution of MCH containing neurons overlaps with that of Hcrt neurons.

Suvorexant blocks morphine changes to Hcrt neurons

We reported that humans with HUD and mice given 50 mg kg^{-1} of morphine daily for 14 or more days have a greatly increased number of detected Hcrt neurons and that the soma size of these Hcrt neurons is greatly decreased[8] (Fig. 1a–c). Although the dual Hcrt receptor antagonist suvorexant (30 mg kg^{-1} in 0.5% methyl cellulose vehicle by gavage (PO), 60 min before morphine) had no significant effect on Hcrt cell number in mice (Fig. 3a, compare vehicle (green) and suvorexant (yellow), $P = 0.548$, Tukey post hoc), suvorexant given 60 min before each daily morphine (50 mg kg^{-1}, SC) injection for 14 days completely prevented the opioid associated increase in the number of Hcrt neurons elicited by morphine (Fig. 3a, vehicle (green) versus morphine (blue), $P < 0.001$; morphine (blue) versus suvorexant + morphine (red), $P < 0.001$, all tests Tukey post hoc).

Similarly, while suvorexant in vehicle by itself had no effect on Hcrt cell size (Fig. 3b, compare vehicle (green) and suvorexant (yellow), $P = 0.988$, Tukey post hoc), suvorexant prevented the reduction in Hcrt soma size produced by morphine (Fig. 3b, compare vehicle (green) versus morphine (blue), $P = 0.004$; morphine versus suvorexant, $P = 0.009$; morphine versus suvorexant + morphine (red), $P < 0.001$, all tests Tukey post hoc).

Suvorexant blocks morphine-induced microglial activation

OUD is known to be linked to microglial activation[33]. Considering the morphological changes in Hcrt neurons induced by opioids but
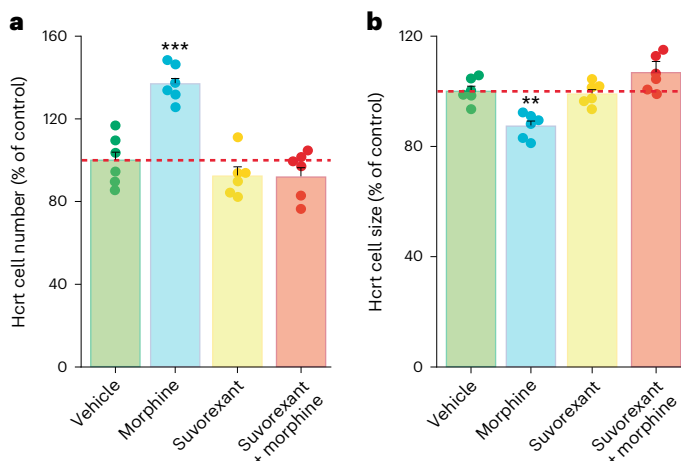
Fig. 3 | Suvorexant blocked changes in Hcrt cell number and size produced by morphine. a,b, Administering suvorexant with morphine completely blocked the increase in Hcrt cell number (morphine versus vehicle, morphine versus suvorexant, morphine versus suvorexant + morphine, all $P < 0.001$, Tukey post hoc, $n = 6$ per condition (**a**)) and the decrease in Hcrt neuronal size (morphine versus vehicle, $P = 0.004$; morphine versus suvorexant, $P = 0.009$; morphine versus suvorexant + morphine, $P < 0.001$, Tukey post hoc, $n = 6$ per condition (**b**)). Suvorexant by itself did not change the number of detected Hcrt neurons or their size ($P = 0.548$ and $P = 0.988$, respectively, compared with vehicle, Tukey post hoc). All data are presented as mean ± s.e.m., and all tests are two tailed. ***$P < 0.001$ and **$P < 0.01$, all conditions compared with morphine.

prevented by concurrent administration of suvorexant, we wondered whether the microglial changes induced by morphine would also be reduced by combining suvorexant with morphine. We were surprised to discover that suvorexant virtually eliminated morphine-induced changes in microglial number and size in the areas we analyzed, that is, suvorexant reduced the microglial inflammatory response to morphine.

Injections of morphine (50 mg kg⁻¹, SC) for 14 days increased the number of hypothalamic Iba-1 labeled microglia and increased hypothalamic microglial soma size compared to the saline condition (Fig. 4a,b, $P = 0.014$ and $P = 0.010$, respectively, Tukey post hoc). Suvorexant (30 mg kg⁻¹, PO) prevented the morphine-induced changes in microglia number and size (Fig. 4a–e). There was no significant difference between hypothalamic microglial number and size in saline versus suvorexant + morphine treated mice (Fig. 4a,b, $P = 0.469$ and $P = 0.950$, respectively, Tukey post hoc).

Similarly, we observed that morphine-treated mice had a significant increase in the number and size of microglial cells in the VTA (Fig. 4f,g, all $P < 0.001$, compared with saline, Tukey post hoc). Suvorexant administration (30 mg kg⁻¹, PO) 60 min before morphine treatment prevented these microglial changes in the VTA (Fig. 4f–j). There was no significant difference in the number and size of microglia comparing saline and suvorexant + morphine in the VTA (Fig. 4f,g, $P = 0.208$ and $P = 0.078$, respectively, Tukey post hoc).

Morphine-induced changes in Hcrt projections to VTA

Daily morphine (50 mg kg⁻¹, SC) for 14 days increased Hcrt axon immunofluorescence intensity in the VTA (Fig. 5a, $P = 0.006$, compared with saline, Tukey post hoc). The increase in intensity was accompanied by a significant increase in Hcrt axonal fiber density (Fig. 5b, $P = 0.003$, compared with saline, Tukey post hoc), comparable to what we have reported in a prior study of the locus coeruleus (LC)[41]. Administration of suvorexant (30 mg kg⁻¹, PO) 60 min before morphine completely blocked the increase in Hcrt axon immunofluorescence intensity in VTA (Fig. 5a, $P = 0.739$, saline versus suvorexant + morphine; $P = 0.017$, compared with morphine alone, Tukey post hoc). This decrease in intensity was accompanied by reduced axonal fiber density (Fig. 5b,

$P = 0.982$, saline versus suvorexant + morphine; $P = 0.002$, compared with morphine alone, Tukey post hoc). Figure 5h shows confocal images of Hcrt fibers in the VTA of mice treated with saline (top), morphine (middle) and suvorexant + morphine (bottom) stained for Hcrt. The difference in Hcrt innervation is visually apparent. Figure 5i shows corresponding Hcrt fiber tracings for each section in Fig. 5h. Figure 5j shows confocal images of the same area stained for TH.

We found that morphine treatment produced a significant increase in TH immunofluorescence in VTA (Fig. 5c,j, compare top and middle, $P = 0.023$, Tukey post hoc), similar to what we have previously described in the LC[41]. We have previously shown that TH immunofluorescence levels have a positive correlation with the amount of TH protein present in the tissue[41]. The increase in TH immunofluorescence in this structure after morphine was accompanied by a significant increase in the number of TH+ neurons detected in morphine treated animals compared with saline (Fig. 5d, $t = 4.337$, d.f. 6, $P = 0.005$, t-test). Suvorexant administration did not significantly affect the morphine-induced increase in TH immunofluorescence intensity (Fig. 5c,j, compare middle and bottom, $P = 0.032$, saline versus suvorexant + morphine; $P = 0.978$, morphine versus suvorexant + morphine, Tukey post hoc).

Although the addiction related structures, LC[41] and VTA[22,23], showed increased Hcrt innervation and TH immunofluorescence after morphine administration, the motor related substantia nigra (SN), adjacent to the VTA and containing a high number of TH+ neurons, was unaffected by morphine treatment. We observed no significant change in Hcrt immunofluorescence intensity in SN (Fig. 5e, $t = 0.372$, d.f. 6, $P = 0.723$, t-test), TH immunofluorescent intensity (Fig. 5f, $t = 0.748$, d.f. 6, $P = 0.483$, t-test) or TH+ cell number (Fig. 5g, $t = 1.076$, d.f. 6, $P = 0.323$, t-test) after chronic morphine administration.

Suvorexant on morphine anticipation and withdrawal

Figure 6a shows wheel running averaged over the last 12 days of the 14 day study periods for three groups. Anticipatory wheel running before morphine administration (gray fill) is seen in the vehicle + morphine group at zeitgeber time (ZT) 2 to 5 (ZT2–ZT5; blue line, V + M). Anticipatory wheel running starts at ZT2 (2 h after the light on pulse), 3 h before the next scheduled daily morphine injection (at ZT5). Anticipatory running continued to ZT5. We observed that anticipatory wheel running began by day 3 as a result of the prior 2 days morphine injections[42,43]. This anticipation was absent in the suvorexant + morphine group (red line, S + M), which received suvorexant 1 h before the morphine dose 21 h earlier, suggesting that is the presence of suvorexant at the time of morphine injection that prevents formation of the anticipatory behavior. Wheel running in both groups further increased at ZT5 after morphine injection.

There was an increase in running in both morphine groups after the mice were handled at ZT4 for vehicle or suvorexant administration. However, the increase of activity at ZT4 after suvorexant (of the suvorexant + morphine group, red line) did not persist whereas the increase of activity after vehicle (of the vehicle + morphine group, blue line) continued. Suvorexant also greatly reduced running after morphine injection at ZT5–ZT10 (red line) compared with the vehicle-then-morphine group, indicating a major dampening by suvorexant on both morphine anticipation and on morphine-induced motor excitation. The green line, S + S, shows the lack of anticipatory activity in the suvorexant + saline group, which experienced the same handling as the other groups but was not given morphine.

We ran these conditions with both 5 mg kg⁻¹ and 10 mg kg⁻¹ doses of morphine with a similar pattern of activity in both experiments (the 5 mg kg⁻¹ dose is shown in Fig. 6a,b). Bar graphs (Fig. 6b–e) indicate total activity during two ZT intervals (ZT2–ZT5 (Fig. 6b,d) and ZT5–ZT10 (Fig. 6c,e)) for each of the two morphine doses used. Animals in the vehicle + morphine group showed anticipatory wheel running activity (Fig. 6b,d, ZT2–ZT5, compare vehicle + morphine
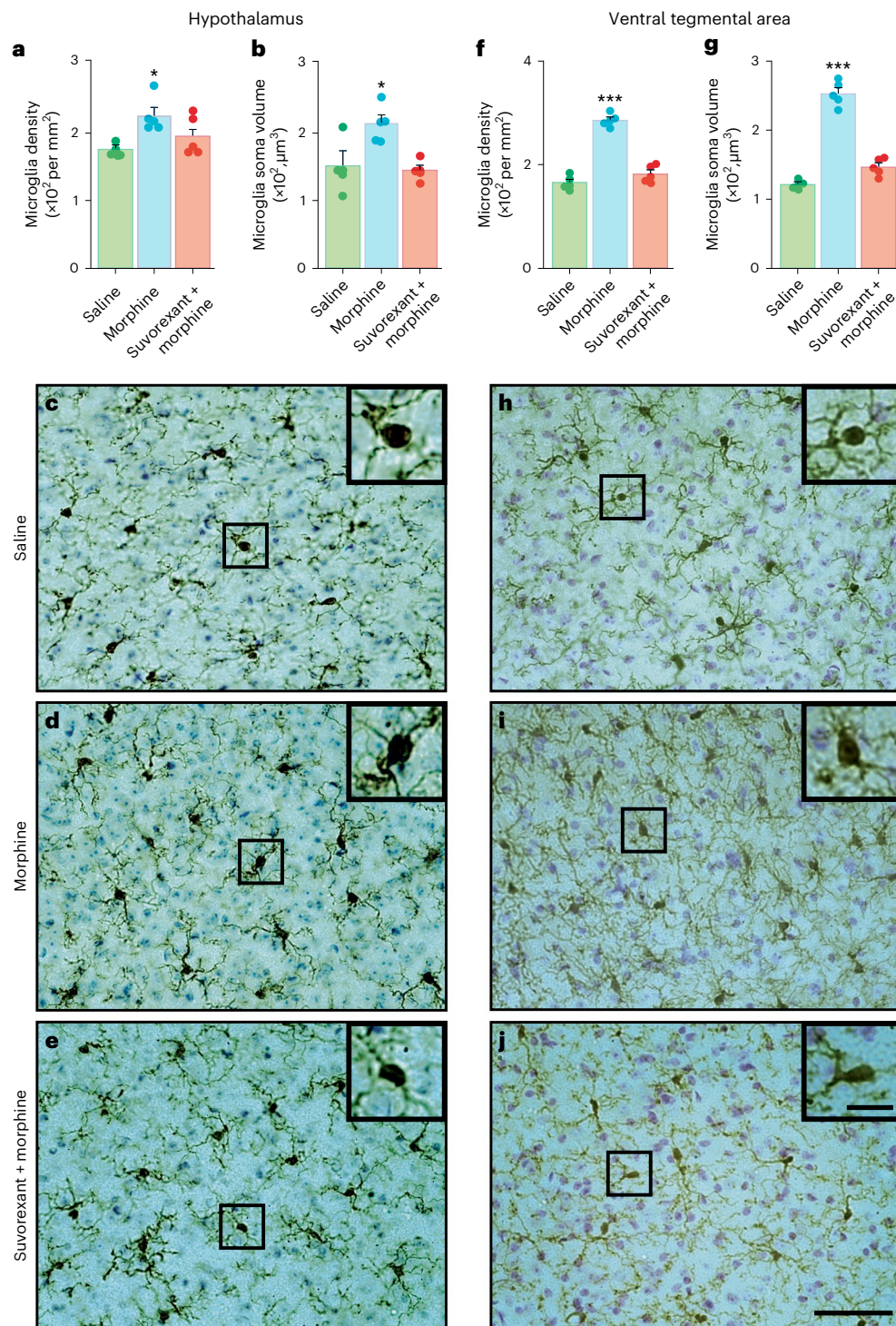
Fig. 4 | Suvorexant blocked microglial activation in the hypothalamus and VTA. a,b, The number (**a**) and size (**b**) of hypothalamic microglia were increased by morphine (50 mg kg^{-1}, 14 days ($P = 0.014$ and $P = 0.010$, respectively, Tukey post hoc compared with saline, $n = 5$ per condition)). Suvorexant (30 mg kg^{-1}), 60 min before morphine, blocked these effects ($P = 0.469$ and $P = 0.950$, respectively for number and size compared with saline condition, Tukey post hoc, $n = 5$ per condition). **c–e,** Hypothalamic sections stained for Iba-1 from saline (**c**), morphine (**d**) or suvorexant + morphine (**e**). The insets are higher magnification (×40) photomicrographs of the selected area (black square) for each condition, illustrating individual microglial cells from animals treated with saline, morphine or suvorexant + morphine. Microglia were easily identified by

their brown coloring and characteristic branching pattern. Hematoxylin-positive nuclei in the background are recognized by their blue–purple color. All data are presented as mean ± s.e.m. and all tests are two tailed. **f,g,** The number (**f**) and size (**g**) of VTA microglia were increased by morphine (50 mg kg^{-1}, 14 days, compared with saline, all $P < 0.001$ Tukey post hoc, $n = 5$ per condition). Suvorexant (30 mg kg^{-1}), 60 min before morphine, eliminated these effects ($P = 0.208$ and $P = 0.078$, respectively, for number and size, compared with saline condition, Tukey post hoc, $n = 5$ per condition). **h–j,** VTA sections stained for Iba-1 from animals with either saline (**h**), morphine (**i**) or suvorexant + morphine (**j**). Scale bar, 50 μm; inset, 10 μm. All data are presented as mean ± s.e.m. and all tests are two tailed. *$P < 0.05$ and ***$P < 0.001$, all conditions compared with morphine.
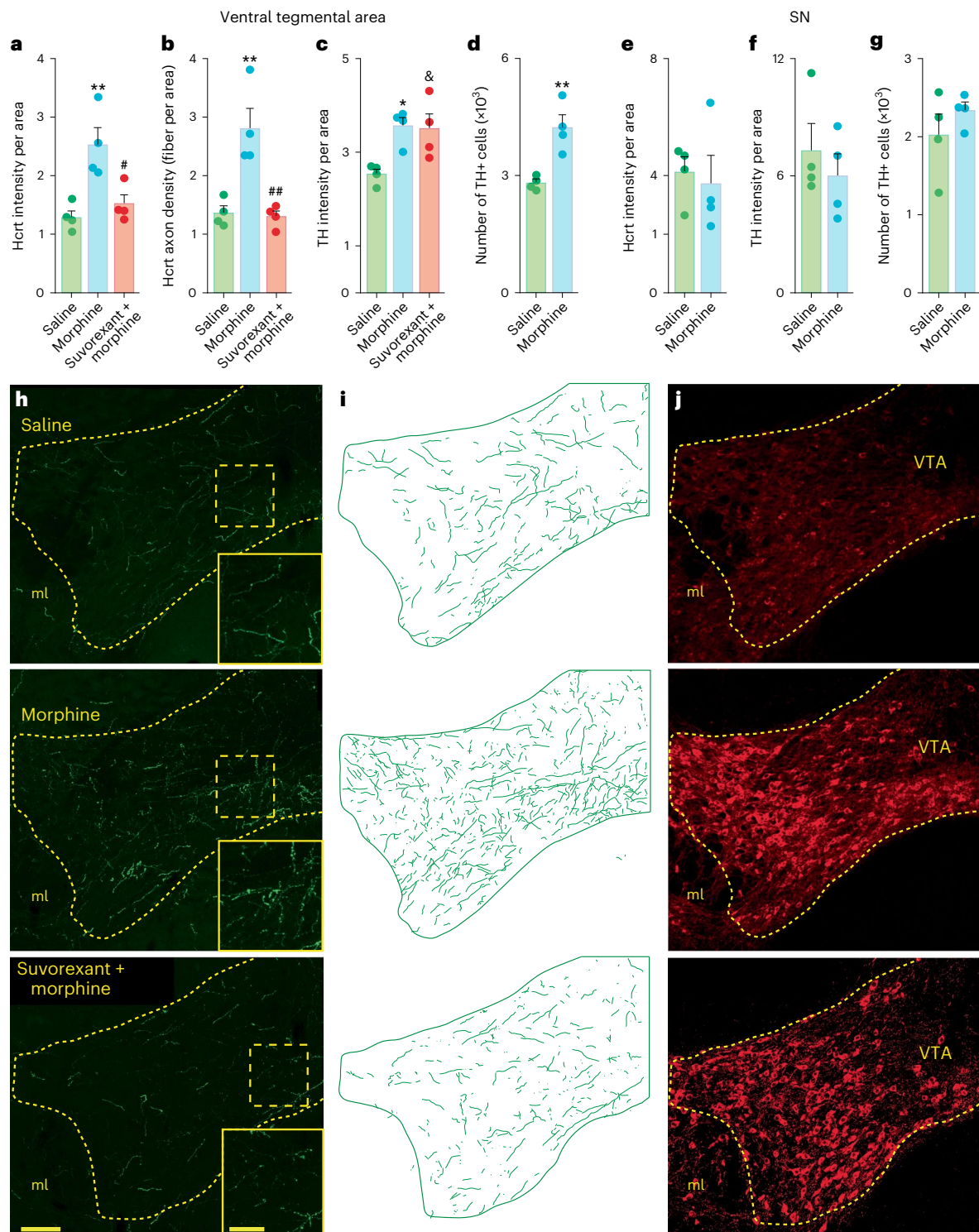
Fig. 5 | Effect of chronic morphine on Hcrt projections, TH levels and TH cell number in VTA and SN. a,b, Morphine (daily, 14 days, 50 mg kg⁻¹, SC) increased Hcrt immunofluorescence intensity (IF) (**a**) in the VTA and increased the density of Hcrt axons in this structure (**b**) (saline versus morphine, $P = 0.006$ and $P = 0.003$, respectively, Tukey post hoc, $n = 4$ per condition). Suvorexant (30 mg kg⁻¹), 60 min before morphine, completely blocked these increases (saline versus suvorexant + morphine, $P = 0.739$, morphine versus suvorexant + morphine, $P = 0.017$, for Hcrt IF; saline versus suvorexant + morphine, $P = 0.982$, morphine versus suvorexant + morphine, $P = 0.002$, for Hcrt axon density, Tukey post hoc, $n = 4$ per condition). **c,** TH IF was increased in morphine compared with saline treatment (saline versus morphine, $P = 0.023$, Tukey post hoc, $n = 4$ per condition). Suvorexant had no effect in the morphine-induced TH level increase (saline versus suvorexant + morphine, $P = 0.032$, morphine versus suvorexant + morphine, $P = 0.978$, Tukey post hoc,

$n = 4$ per condition). **d,** Morphine-treated animals showed an increase in the number of TH+ neurons in the VTA ($t = 4.35$, d.f. 6, $P = 0.005$, t-test, $n = 4$ per condition). **e–g,** Adjacent SN showed no change in Hcrt IF (**e**) ($t = 0.723$, d.f. 6, $P = 0.723$, t-test, $n = 4$ per condition) or TH IF (**f**) ($t = 0.748$, d.f. 6, $P = 0.483$, t-test, $n = 4$ per condition) and no change in the number of TH+ neurons (**g**) ($t = 1.076$, d.f. 6, $P = 0.323$, t-test, $n = 4$ per condition) after morphine. All data presented as mean ± s.e.m. and all tests are two tailed. **h,** Representative images of animals treated with saline (top), morphine (middle) and suvorexant + morphine (bottom) stained for Hcrt. The difference in Hcrt innervation is visually apparent. **i,** Corresponding Hcrt fiber tracings for each section. **j,** Confocal images of the same area stained for TH. Scale bar, 100 μm; inset, 20 μm. ml, medial lemniscus. *$P < 0.05$, **$P < 0.01$, morphine versus saline; #$P < 0.05$, ##$P < 0.01$; morphine versus suvorexant + morphine; &$P < 0.05$, saline versus suvorexant + morphine.

versus suvorexant + saline, all $P < 0.001$ for either morphine dose, Tukey post hoc). Suvorexant blocked the anticipatory activity (ZT2–ZT5) induced by morphine (Fig. 6b,d, compare suvorexant + morphine versus vehicle + morphine condition, $P = 0.003$ and $P < 0.001$ for 5 mg kg^{-1} and 10 mg kg^{-1} morphine dose, respectively, Tukey post hoc). Activity during ZT2–ZT5 did not differ between suvorexant + morphine and suvorexant + saline groups ($P = 0.541$ and $P = 0.118$ for 5 mg kg^{-1} and 10 mg kg^{-1} morphine doses, respectively, Tukey post hoc). Suvorexant also reduced morphine-induced hyperactivity (ZT5–ZT10) (Fig. 6c,e, $P < 0.001$ and $P = 0.011$ for 5 mg kg^{-1} and 10 mg kg^{-1} morphine doses, respectively, Tukey post hoc).

In another set of animals, we sought to determine whether administration of suvorexant with morphine would affect the symptoms of opioid withdrawal induced by opioid receptor antagonist naloxone in morphine dependent animals. Figure 6f shows that blocking Hcrt receptors with suvorexant 60 min before daily morphine administration for 14 days significantly reduced the global somatic signs of opioid withdrawal caused by injection of naloxone in mice that had been administered morphine (compare vehicle + morphine versus suvorexant + morphine, $t = 2.847$, d.f. 9, $P = 0.019$, t-test).

Suvorexant does not decrease morphine analgesia

We tested the effect of suvorexant on the pain threshold using an IITC PE34 Incremental Thermal Nociceptive Threshold Analgesia Meter (IITC Life Science Inc.). The analgesic effect of morphine (that is, elevation of nociceptive threshold) on the paw raising response to floor heating is apparent comparing vehicle alone to vehicle + morphine (Fig. 6g,h, $P = 0.004$ and $P < 0.001$ for 5 mg kg^{-1} and 10 mg kg^{-1} morphine doses, respectively, Tukey post hoc). The average analgesic effect ($n = 6$ per group, 3 tests) was not significantly diminished by the 30 mg kg^{-1} oral dose of suvorexant (actually suvorexant nonsignificantly increased analgesia) after either 5 mg kg^{-1} or 10 mg kg^{-1} morphine doses (compare vehicle + morphine versus suvorexant + morphine, $P = 0.962$ and $P = 0.947$, respectively, Tukey post hoc). The suvorexant + morphine (5 mg kg^{-1} and 10 mg kg^{-1}) analgesic effects versus vehicle were significant ($P = 0.002$ and $P < 0.001$, respectively, Tukey post hoc). The suvorexant dosage (30 mg kg^{-1}) that preserved opioid analgesia is the same as that which completely prevented the chronic morphine associated increase in Hcrt cell number and decrease in size seen in Fig. 3, the microglial activation seen in Fig. 4, the increase in Hcrt axonal density in the VTA seen in Fig. 5 and the morphine anticipation and reduced morphine withdrawal symptoms seen in Fig. 6.

Discussion

As shown in ref. 8 and in Fig. 1, long-term self-administration of heroin in humans or administration of addictive levels of morphine to mice produced an increase in the number of detected Hcrt neurons and decrease in the size of Hcrt neurons. A 44% increase in the number of Hcrt neurons was observed after administration of colchicine, an inhibitor of microtubule polymerization that prevents transport of peptides out of the cell soma and thereby increases the amount of Hcrt in Hcrt producing neurons[40] (Fig. 2). This suggests that Hcrt expression in a subpopulation of Hcrt neurons is below the detection level under baseline conditions, with 44% of Hcrt expressing neurons being undetectable. The percentage increase in the number of detected Hcrt neurons after colchicine is comparable in magnitude to the increase in the number of Hcrt neurons produced by chronic self-administration of heroin in humans or administration of morphine or fentanyl to naive mice or rats[8,9]. We show that co-administration of morphine with the opioid antagonist naltrexone prevents the morphine-induced changes in number and size of Hcrt neurons, confirming, not surprisingly, that opioid receptor activation is required for these opioid effects.

Administration of both morphine and colchicine does not increase the number of Hcrt neurons beyond that produced by colchicine alone, indicating that the morphine-induced increase in the number of Hcrt-labeled neurons does not result from neurotransmitter respecification, that is, does not cause non-Hcrt neurons to start synthesizing Hcrt, and indicates a ceiling effect of morphine on Hcrt neuronal number[39,44]. However, in contrast to what we observed in the Hcrt neuronal population, the total number of MCH neurons remained unchanged by colchicine administration, although colchicine enhanced the immunostaining intensity of both Hcrt and MCH cell populations in a comparable manner (Fig. 2). Similarly, colchicine does not affect the number of somatostatin-expressing neurons, another neuronal group located in the hypothalamus[40]. We have previously reported that MCH neuronal numbers remained stable as a function of time of day[45], and are unaffected by morphine, fentanyl or cocaine administration[8–10]. In contrast, detected Hcrt neuronal cell number significantly varies as a function of time of day[45] and as a function of morphine, fentanyl and cocaine administration[8–10]. We hypothesize that the difference in colchicine effects lies in the relatively constant, detectable expression of intracellular MCH, whereas 44% of Hcrt expressing neurons have Hcrt levels that fall below the current detection threshold under baseline conditions. The increase in Hcrt peptide levels in colchicine- or morphine-treated animals makes undetected Hcrt neurons detectable. The stability of MCH neuronal number after

Fig. 6 | Hcrt receptor blockade prevents conditioned morphine anticipation of daily morphine injection. a, Vertical yellow bars on left and right indicate the beginning and the end of the 'skeleton light period'. We studied three groups of 6 mice per group given 5 mg kg^{-1} of morphine, and a second cohort of 3 groups of 6 mice per group, given 10 mg kg^{-1} of morphine (a total of 36 mice). Groups were given vehicle (0.5% methyl cellulose PO) with or without suvorexant (30 mg kg^{-1}) at ZT4, followed by morphine or saline at ZT5. The time course of activity of the 5 mg kg^{-1} group is shown in **a**. Anticipatory wheel running (gray fill) is seen in the 'vehicle at ZT4 then morphine at ZT5 group' under the blue line starting at ZT2 (2 h after the light on pulse, which is 21 h after the last morphine dose, given on the prior day). The anticipatory running continues until ZT5. Running further increased at ZT5 after morphine injection. The anticipatory running was absent in the group given suvorexant before morphine (red line). The group given suvorexant followed by saline, but no morphine (green line), also showed no anticipatory running. **b–e**, The total activity during two ZT intervals (ZT2–ZT5 and ZT5–ZT10) for each of the two morphine doses. **b**, At 5 mg kg^{-1} at ZT2–ZT5 (V + M versus S + S, $P < 0.001$; V + M versus S + M, $P = 0.003$; S + M versus S + S, $P = 0.541$, Tukey post hoc, $n = 6$ per condition). **c**, At 5 mg kg^{-1} at ZT5–ZT10 (V + M versus S + S, $P < 0.001$; V + M versus S + M, $P < 0.001$; S + M versus S + S, $P = 0.002$, Tukey post hoc, $n = 6$ per condition). **d**, At 10 mg kg^{-1} at ZT2–ZT5 (V + M versus S + S, $P < 0.001$; V + M versus S + M, $P = 0.001$; S + M versus S + S, $P = 0.118$, Tukey post hoc, $n = 6$ per condition). **e**, At 10 mg kg^{-1} at ZT5–ZT10 (V + M versus S + S,

$P < 0.001$; V + M versus S + M, $P = 0.011$; S + M versus S + S, $P < 0.001$, Tukey post hoc, $n = 6$ per condition). All data presented as mean ± s.e.m. and all tests are two tailed. *$P < 0.02$, **$P < 0.01$ and ***$P < 0.001$, compared with vehicle + morphine group. **f**, Suvorexant administration 60 min before morphine (50 mg kg^{-1}, 14 days, SC, $n = 6$) reduced the global somatic signs of naloxone-induced opioid withdrawal in morphine-dependent animals (vehicle + morphine group, $n = 5$). The difference was significant ($t = 2.847$, d.f. 9, $P = 0.019$, t-test). Data are presented as mean ± s.e.m. and all tests are two tailed. *$P < 0.02$. **g,h**, The analgesic effect of morphine on the delayed paw raising response to floor heating expressed as the increase in nociception threshold. The analgesic elevation of nociceptive threshold to heat was evident after morphine ($P = 0.004$ and $P < 0.001$, comparing vehicle + morphine with vehicle alone for 5 mg kg^{-1} and 10 mg kg^{-1}, Tukey post hoc, $n = 6$ per condition). Analgesia was not significantly diminished by 30 mg kg^{-1} of suvorexant in both 5 mg kg^{-1} and 10 mg kg^{-1} morphine doses (actually, suvorexant nonsignificantly increased analgesia at both doses) after both 5 mg kg^{-1} or 10 mg kg^{-1} morphine doses ($P = 0.962$ and $P = 0.947$, Tukey post hoc comparisons between vehicle + morphine and suvorexant + morphine of either dose, $n = 6$ per condition). The suvorexant + morphine (5 mg kg^{-1} and 10 mg kg^{-1}) analgesic effect was significant with respect to vehicle ($P = 0.002$ and $P < 0.001$, respectively, Tukey post hoc, $n = 6$ per condition). All data presented as mean ± s.e.m. and all tests are two tailed. **$P < 0.01$ and ***$P < 0.005$, compared with vehicle condition.

opioid administration may be related to the absence of mu opioid receptors in these neurons[46].

Hcrt neurons are excited when animals are administered morphine or cocaine in vivo[8,10] and neuronal excitation has been previously associated with modifications in synthesis pathways[47,48]. Since Hcrt neurons express Hcrt receptor 2 (HcrtR2) and are directly excited by Hcrt peptides[49], we wanted to determine whether blocking Hcrt receptors might affect the increase in the number and shrinkage of detected Hcrt neurons produced by opioids. We found that administration of the dual Hcrt receptor antagonist suvorexant completely prevented the
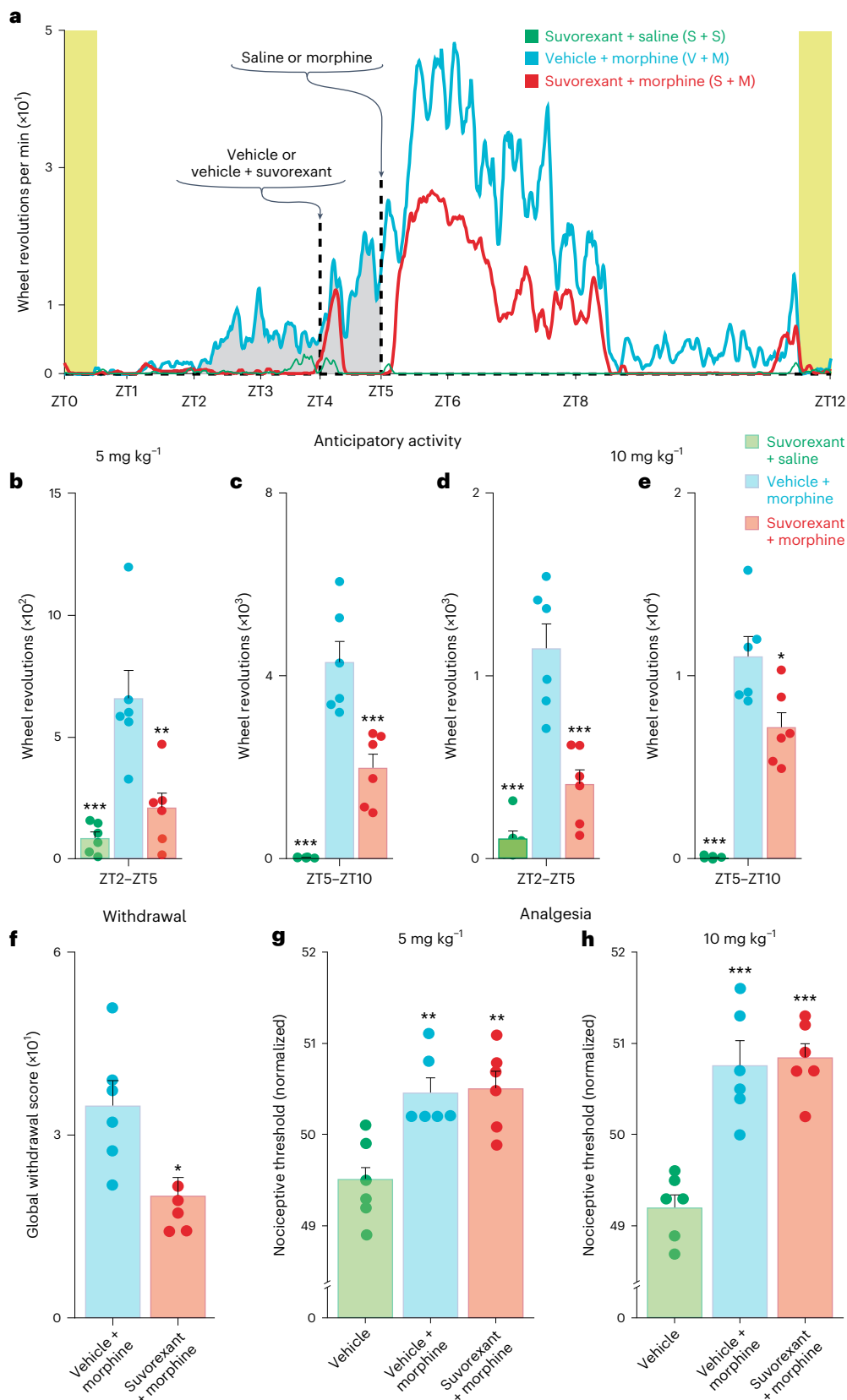
increase in number and the decrease in size of Hcrt neurons produced by chronic opioid administration (Fig. 3). The effects of suvorexant on Hcrt neurons are probably mediated by a combination of direct and indirect pathways. Suvorexant will directly block Hcrt receptors present on Hcrt neurons decreasing the excitability of these cells. An indirect pathway would result from the summation of suvorexant effects in all neuronal inputs to Hcrt neurons. In vitro experiments using heterologous expressing cell lines have shown that HcrtR1 and kappa opioid receptors can heterodimerize and that the cross-talk between these receptors can modulate their activity[50]. Receptor interactions may contribute to the anatomical changes we describe.

Exposure to opioids elicits neuroinflammation as evidenced by the activation of microglia, and is associated with the development and maintenance of OUD[32]. Our results indicate that daily morphine exposure leads to microglial activation in the Hcrt-containing region of the hypothalamus and in the VTA (Fig. 4). Microglia can be directly modulated by Hcrt and opioids since they express both types of receptors[36,37]. Here, we report that pretreatment with the dual Hcrt receptor antagonist suvorexant completely prevents morphine-induced microglial activation in these structures, indicating a critical role of Hcrt in the modulation of the microglial response to opioids. Reduction of neuroinflammation by suvorexant may be an important factor in preventing the changes in Hcrt neuron number and size, in blocking opioid anticipatory wheel running and in the reduction of opioid withdrawal symptoms in morphine dependent animals that we report here.

In a prior work we showed that chronic morphine administration resulted in a significant increase in Hcrt neuronal projections to the LC[41]. We now show that 50 mg kg^{-1} of morphine for 14 days also increases Hcrt axonal density in the VTA, a region that has been strongly implicated in OUD[22,23] (Fig. 5). We cannot yet determine whether the new Hcrt axons detected in the VTA region originate from the entire Hcrt population seen under baseline conditions or from the undetected Hcrt neurons that become visible after morphine administration. The VTA receives extensive projections from Hcrt neurons, but less than 5% of Hcrt axons have specialized synaptic connections to VTA neurons[28], suggesting that Hcrt action on VTA is predominantly extrasynaptic. We speculate that the increase in Hcrt axonal density in this area results in higher Hcrt levels that increase the activity of VTA neurons. Hcrt excitation of DA neurons may increase DA efflux in reward related target areas such as the NAc[26,27].

In parallel with the blocking effects of suvorexant on the morphine-induced increase in Hcrt neuronal numbers, we found that the increase in Hcrt axonal density in the VTA is also blocked in animals pretreated with suvorexant before morphine. In contrast, we find that Hcrt projections to the substantia nigra, a TH+ region adjacent to the VTA but not generally implicated in OUD, are not significantly increased by morphine administration, suggesting that opioid effects on Hcrt projections are regulated in a target-specific manner.

These anatomical findings led us to test the effect of suvorexant on morphine anticipation, morphine withdrawal and morphine analgesia (Fig. 6). To measure anticipation, we used a wheel running model of anticipation of addictive drug administration[42,43,51,52]. After 2 days of daily injection of morphine at ZT5, mice anticipated the daily injections by vigorous wheel running starting at ZT2, at morphine doses as low as 5 mg kg^{-1}. However, when morphine injections were preceded by suvorexant administration no anticipatory wheel running occurred. Note that the anticipation was occurring 21 h after the prior morphine injection, and 3 h before the next morphine injection, at a time when minimal amounts of morphine or suvorexant would be present. It seems likely that it was the presence of suvorexant at the time that morphine was injected that prevented the conditioned anticipatory running manifested 21 h later. The suvorexant effect on morphine anticipation may be a result of the blockade of self-excitation of the Hcrt neuronal population[49] combined with effects on indirect pathways.

At the suvorexant dose used, even though given in the 'skeleton light period' (Methods), the normal mouse sleep period, no sleep occurred for at least 3 h in either the mice given morphine or the mice given suvorexant + morphine, as evidenced by wheel running quantification (Fig. 6) and video observation. This is due to the well-known arousing quality of opioids in mice and rats[53]. Therefore, even though suvorexant is a 'sleeping pill' at certain doses in humans (the dual Hcrt receptor antagonist suvorexant is marketed as Belsomra, with newer dual Hcrt receptor antagonists daridorexant in Quviviq and lemborexant in Dayvigo), sleep induction did not mediate the observed effect of suvorexant on morphine-induced changes in Hcrt cell number and size shown in Figs. 1 and 3. It is useful to recall that morphine itself is soporific in humans, which is why morphine was named after Morpheus, that is, sleepiness does not prevent the opioid addictive process, but suvorexant does.

We found that blocking Hcrt receptors before morphine administration significantly reduced the somatic signs of pharmacologically (naloxone) induced withdrawal in mice administered morphine for 14 days (Fig. 6f). This result is consistent with our prior report[41] showing that elimination of Hcrt neurons in adult mice greatly reduced the behavioral signs of opioid withdrawal in morphine-dependent animals. Taken together, these results support the idea that Hcrt system plays a critical role in the symptoms of opioid addiction.

Blocking Hcrt receptors with suvorexant before morphine administration prevented the addiction-associated anatomical changes in Hcrt neuron number, size, Hcrt axonal projections to the VTA and microglial activation (Figs. 3–5). Behaviorally, suvorexant completely blocked morphine anticipatory motor activation and significantly reduced the somatic signs of opioid withdrawal triggered by naloxone administration. However, we find that opioid analgesia is not at all diminished by suvorexant (Fig. 6g,h).

Conclusion

These findings suggest an important role of the Hcrt system in the anatomical and behavioral response to chronic opioid exposure. We speculate that co-administration of suvorexant, or other Hcrt receptor antagonists, to human patients treated with opioids for pain relief would greatly reduce the potential for developing OUD. Human trials are necessary to test the effectiveness of this approach.

Methodological considerations

We and others have shown that the number of immunohistochemically detected cells in animals of the same age and genetic background may vary as a function of tissue processing, the antibody used or the method of data collection[54–57]. To minimize sources of experimental variability we processed all subjects for each experiment using the same procedure including all solutions and antibody lot number. Our prior work indicates that the level of Hcrt production can fall below the detection of immunohistochemical technique[45], with nondetection not necessarily an indication of the complete absence of Hcrt.

An alternative method to visualize cells in tissue samples is the detection of specific messenger RNAs by in situ hybridization. However, the presence of a particular mRNA in a cell does not guarantee the expression of the encoded molecule. In addition, in narcoleptic patients for example, in situ hybridization can fail to detect the appropriate prepro Hcrt mRNA[7], despite the presence of Hcrt neurons (10%) confirmed by immunohistochemistry[6,58].

In our human studies, we included male and female individuals and observed that the increase in the number and decrease in size of hypocretin neurons was similar[8]. This suggested that the hypocretin system responds in a similar manner to chronic opioid exposure in both biologically assigned sexes. On the other hand, in our animal studies we used male mice. There is still no clear consensus regarding the effects of opioids between male and female rodents[59]. Human clinical studies in both males and females are necessary.

Methods

Human tissue

Immunohistochemistry was used to stain for hypocretin (orexin) in human brain tissue from neurologically normal controls and humans with HUD. Human brain tissue was obtained from the National Neurological Specimen Bank Eunice Kennedy Shriver National Institute of Child Health and Human Development Brain Bank.

Animal usage

All procedures were approved by the Institutional Animal Care and Use Committees of the University of California at Los Angeles and of the Veterans Administration Greater Los Angeles Health Care Systems: 08013-14 and 1761605. Experiments were performed in C57BL/6 male mice and animals were randomly assigned to the different experimental groups. A total of 170 mice were used in the current study. All experimental procedures were started when animals reached 3 months of age. Animals were kept in a room maintained at $22 \pm 1\,°C$ on a 12-h light (135 lux) dark (0.03 lux) cycle (lights on at 6 AM and off at 6 PM) or on a 'skeleton' light schedule as described below.

Drugs

Morphine sulfate (Hospira Inc.) 5, 10 and 50 mg kg^{-1}, naltrexone hydrochloride (Sigma-Aldrich, N3136) 50 mg kg^{-1} and naloxone (naloxone hydrochloride dihydrate, N7758, Millipore Sigma) 2 mg kg^{-1} were used. Morphine was diluted with sterile saline (sodium chloride injection, US Pharmacopeia, 63323-186-10, APP pharmaceuticals) and naltrexone and naloxone were dissolved in sterile saline immediately before SC administration. Suvorexant (Belsomra) was suspended in 0.5% methyl cellulose (M0262, Sigma-Aldrich) in water and orally administered by gavage.

Tissue processing

Animals were anesthetized intraperitoneally (i.p.) with Fatal-Plus pentobarbital solution (150 mg kg^{-1}, Vortech Pharmaceuticals) and then perfused transcardially with 0.035 l heparinized (1,000 units l^{-1}, heparin sodium injection, 63739-953-25, Aurobindo Pharma Limited) phosphate-buffered saline ((PBS) 0.1 M, pH 7.4: sodium phosphate dibasic, 0404.2.5, Avantor; sodium phosphate mono basic, EC231-449-2, Fisher Scientific; sodium chloride, S671-3, Fisher Scientific), followed by 4% paraformaldehyde (P6148-5, Sigma-Aldrich) in PBS. Brains were removed and post-fixed for 72 h in 4% paraformaldehyde in PBS, followed by 20% sucrose (S5-12, Fisher Scientific) in PBS for 24 h and 30% for 48 h. Brains were frozen and cut into 40-μm coronal sections using a sliding microtome (American Optical). The sections were sorted into one in three-well compartments containing PBS. Immunohistochemical procedures were performed immediately. The remaining tissue was transferred to a cryoprotectant solution, consisting of a mixture of 30% ethylene glycol (BP 230-4, Fisher Scientific) and 25% glycerol (BP229-1, Fisher Scientific) in PBS, and stored at −20 °C. Mice that we compared were always killed and processed together. Perfusion, histology and analysis of microscope sections were performed by investigators blind to the procedures performed prior to sacrifice.

Immunostaining for brightfield microscopy

Experimental procedures were conducted in male, C57BL/6 mice, 3 months old. For the anatomical studies of chronic morphine exposure and opioid antagonists, $n = 16$ ($n = 4$ per condition) mice were used; for the colchicine studies, $n = 20$ were used (for details of individual experimental group see colchicine procedure below) and for microglial studies, $n = 10$ were used. All immunohistochemical procedures were performed by sequential incubation of free-floating sections. For detection of Hcrt and MCH, sections were first incubated for 30 min in 0.5% hydrogen peroxide (5240-02, Macron Fine Chemicals) in PBS to block endogenous peroxidase activity. After thorough washing with PBS, the sections were placed for 2 h in 1.5% normal goat serum

((NGS) 005-000-121, Jackson ImmunoResearch Laboratories) in PBS containing 0.25% Triton X ((PBST) T8787, Sigma-Aldrich, lot #SLCJ 6163) and incubated for 72 h at 4 °C in a PBST solution containing rabbit anti-Hcrt-1 primary antibody (1:10,000, H-003-30, lot #01108, Phoenix Pharmaceuticals Inc., Burlingame, CA, USA) or rabbit anti-MCH (1:20,000, H-070-47, Lot # 01629-5, Phoenix Pharmaceuticals Inc.), followed by the corresponding biotinylated secondary antibody (1:400, PK-6101, Vector Laboratories) in PBST for 2 h, and avidin–biotin–peroxidase complex (1:300, ABC Elite Kit, Vector Laboratories) in PBS for 2 h. The tissue-bound peroxidase was then developed using the diaminobenzidine tetrahydrochloride ((DAB) SK4100, Vector Laboratories) method, which consisted of tissue immersion in 0.02% DAB and 0.03% hydrogen peroxide in 10 ml PBS.

We previously standardized our DAB method and established an 8-min optimal developing time and used this precise duration in all of our studies. All developing solutions were prepared in one container, homogenized and aliquoted to the respective developing wells. Developing procedures were performed with room lights off and the wells containing tissue were wrapped with aluminum foil to prevent light exposure. Wells were agitated at 55 r.p.m. Developing solutions were used only once.

Microglia ($n = 5$ per condition) were identified using the canonical marker, ionized calcium binding adapter molecule-1 (Iba-1)[60]. Before Iba-1 immunostaining, an antigen retrieval procedure was performed by incubating the sections in 10 mM sodium citrate (S279-500, Fisher Scientific) (pH 8.5) at 80 °C for 30 min. The sections were then cooled to room temperature in sodium citrate, washed with PBS and, following the same staining procedures used to detect Hcrt-1, using primary antibody goat anti-Iba-1 (ab5076, Abcam, lot #GR3403958, 1:10,000) and normal rabbit serum (PK6105, Vector Laboratories). Sections were mounted on slides and counterstained for the identification of anatomical landmarks, according to the following procedures. Slides were placed in distilled water, followed by hematoxylin solution (FD hematoxylin solution, PS104-02, FD Neurotechnologies). They were then briefly rinsed in tap water, followed by distilled water containing 2% glacial acetic acid (8507-500, Fisher Scientific).

The number, distribution and size of Hcrt+ and Ibal-1+ cells and the number and distribution of MCH+ cells were assessed using a Nikon Eclipse 80i microscope with a three-axis motorized stage, video camera, Neurolucida interface and Stereoinvestigator software (MicroBrightField Corp.). Cell counting was performed bilaterally using either 40× or 60× objective and cell size was determined using the Neurolucida Nucleator probe. Iba-1+ quantification was performed bilaterally in the middle of the Hcrt neuronal field by placing a square (250 μm × 250 μm) dorsal to the fornix, with the lower corners of the square equidistant from the center of the fornix. Quantification of Iba-1+ cells was performed bilaterally in the same manner in the VTA, by placing a square (250 μm × 250 μm) medial to the medial lemniscus. All counting and cell measurements were performed by a trained histologist, always blind to the experimental condition. In every case, the same individual counted both the experimental and control tissue. Only neurons with an identifiable nucleus were counted.

The number of animals used in each experiment is as follows: Fig. 1b–e, $n = 4$ per condition; Fig. 2, $n = 4$ per condition; Fig. 3, $n = 6$ per condition; Fig. 4, $n = 5$ per condition.

Immunostaining for confocal microscopy

All experimental procedures were conducted in male, C57BL/6 mice, 3 months old. An $n = 4$ was used for each experimental condition. For identification of DA-containing neurons in the VTA and SN regions, we used the immunohistochemical detection of the TH enzyme. The sections were first incubated in PBST containing 1.5% of both NGS and normal donkey serum ((NDS) 017-000-121, Jackson ImmunoResearch Laboratories), followed by co-incubation with primary antibodies rabbit anti-Hcrt-1 (H-003-36, Phoenix Pharmaceuticals, 1:2,000, lot

#01108) and sheep anti-TH (ab113, Abcam, 1:1,000, lot #GR 3277795-15) overnight at room temperature in PBST, 1% NGS and 1% NDS. Next, we washed the sections and incubated them in PBST containing the corresponding secondary antibody tagged with fluorophores that match our microscope filters (1:300, Alexa Fluor 488 goat anti-rabbit, A-11008, lot #2557379, Alexa Fluor 555 donkey anti-sheep, A21436, lot #2420712, Thermo Fisher Scientific), 1% NGS and 1% NDS, with lights off and samples wrapped in aluminum foil. Tissue was mounted and cover slipped using Vector Shield anti-fade mounting media (H 1000, Vector Laboratories). All tissue sections from experimental and control animals were stained at the same time and with the same antibody lot. To quantify the number of TH+ neurons, the same mounting media containing 4′,6-diamidino-2-phenylindole was used (H 1200, Vector Laboratories). All tissue sections from experimental and control animals were stained at the same time and with the same antibody lot.

The number and distribution of Hcrt fibers and TH+ cell bodies was assessed using a Zeiss LSM 900 (Imager Z2 AX10) confocal microscope equipped with the appropriate lasers. All data collection and analysis was performed by a trained histologist, always blind to the experimental condition. In every case, the same individual counted both the experimental and control tissue. Every section that contained the VTA and adjacent SN was imaged at 1 μm optical planes; 28 ± 1.4 optical planes were obtained per section. Quantification was performed bilaterally on every third section throughout the region of interest. Immunofluorescence intensities and area measurements were obtained using the Zeiss proprietary software ZEN. The area was defined by the size of the region containing TH neuronal bodies in each structure. Total immunofluorescence for TH and Hcrt was divided by the corresponding area, and bilateral areas in the same section were averaged. Cell number and fiber distribution were determined using Adobe Illustrator. Every stack of images was loaded in this program such that each optical plane was placed in a distinct layer and individual TH containing neurons were identified and marked. Using this method of quantification eliminates double counting of cells, which is critical in the analysis of structures with a high density of neuronal bodies such as the VTA and SN.

For the analysis of Hcrt fiber length and distribution, the middle optical plane was chosen for matching sections that contained the VTA. Individual fibers were drawn and measured and the total fiber density was then calculated on the basis of the area used to measure the immunofluorescence intensities.

Colchicine procedure
All experimental procedures were conducted in male, C57BL/6 mice, 3 months old. Two groups of animals ($n = 4$ per group) were subjected to ICV injection of either saline solution or saline solution containing 20 μg μl^{-1} of colchicine (C9754, Sigma-Aldrich), a microtubule disruptor that prevents axonal transport and increases levels of neuropeptides in cell somas[40]. Another two groups of animals ($n = 4$ per group) received 14 days of either saline or morphine (50 mg kg^{-1}) before ICV injections of colchicine. An additional four naive animals served as the control. Anesthesia was induced with a mixture of ketamine (ketamine hydrochloride injection, 0143-9509-10, Hikma Pharmaceuticals) and xylazine (AnaSed 20 injection, 59399-110-20, Akorn Animal Health) (100 mg kg^{-1} and 15 mg kg^{-1}, respectively, i.p.) and then maintained with a gas mixture of isoflurane (Aspen Veterinary Resources, Ltd.) in oxygen (1–3%) after the animals were placed in the stereotaxic device. Body temperature was maintained with a water-circulating heating pad (Gaymar Industries). The head was positioned in a stereotaxic frame and the skull was exposed. A hole was drilled at coordinates corresponding to the lateral ventricle (anterior-posterior −0.5 mm, lateral −1 mm, relative to bregma). A Hamilton microsyringe was lowered until the ventricle was reached (height −2.8 mm, relative to the skull surface). Infusion was made in increments of 0.2 μl every 10 min for 40 min to obtain a final volume of 1 μl. The needle was held in place for

another 10 min before being slowly withdrawn. Ventricular localization was confirmed by observing free-flowing cerebrospinal fluid after the withdrawal of the needle. A small piece of sterile bone wax was placed over the hole and the skin sutured. All subjects recovered from the anesthesia within 30 min after the end of the procedure. Animals were carefully monitored and sacrificed 52 h later between ZT13 and ZT15, following the same tissue processing protocol described above for immunohistochemical procedures.

Morphine anticipation
All experimental procedures were conducted in male, C57BL/6 mice, 3 months old. Running wheels were used to measure conditioned anticipation of morphine administration. This technique has been used to quantify drug anticipation and appetitive changes[42,43,51,52]. We adopted this method for measuring morphine anticipation. Low-profile running wheels for mice (model ENV-047, Med Associates) were placed in the testing cages (length 48.3 cm, width 26.7 cm and height 40.6 cm) for a 2-week adaptation period and were continuously monitored wirelessly. Two days before the beginning of injections animals were placed in a 'skeleton light cycle' (lights on for 30 min at 6:00 AM and on again for 30 min at 6:00 PM) for the duration of the experiment. This lighting schedule disinhibits running wheel behavior during a period in which light would otherwise inhibit wheel running. Running wheel activity was collected and analyzed using Med Associates software (SOF-861). Continuous video monitoring and the wheel running records showed that no sleep occurred for more than 4 h after morphine administration in any mouse.

A total of 36 male mice ($n = 6$ per treatment combination) received 14 days of orally administered suvorexant (30 mg kg^{-1}) or vehicle (0.5% methyl cellulose, PO) at 10:00 AM (ZT4) followed by morphine (5 or 10 mg kg^{-1}, SC) or saline (0.05 ml, SC) at 11:00 AM (ZT5).

Precipitated opioid withdrawal
All experimental procedures were conducted in male, C57BL/6 mice, 3 months old. The procedure started with $n = 6$ in each condition. In the course of the experiment, one individual suffered health complications and had to be killed before the conclusion of the experiment. This animal was excluded from the final analysis. Somatic signs of naloxone precipitated opioid withdrawal in morphine dependent mice have been previously studied using a 5-day escalating dose of morphine (starting with 20 mg kg^{-1} and leading up to 100 mg kg^{-1}). In a prior report[41] we compared the behavioral effects of this dose and schedule of morphine administration with our daily (50 mg kg^{-1}) morphine injection for 14 days. We observed that both drug exposure regimes resulted in a comparable global withdrawal score.

Mice ($n = 11$, 6 vehicle + morphine, 5 suvorexant + morphine) were administered daily vehicle (0.5% methyl cellulose, PO) or suvorexant in vehicle (30 mg kg^{-1}) at 8:00 AM (ZT2) followed by morphine (50 mg kg^{-1}, SC) at 9:00 AM (ZT3) for 14 days. Two hours after the last morphine injection, naloxone (2 mg kg^{-1}, SC) was administered and behavioral withdrawal symptoms were assessed. All sessions were conducted in Plexiglas cages. We quantified locomotion, jumping, backward stepping, rearing, paw tremor, teeth chattering, grooming, behavioral arrest, defecation, urination, wet dog shake, ptosis, diarrhea, body tremor and piloerection. A global withdrawal score was calculated[46,61].

Analgesia measurement
All experimental procedures were conducted in male C57BL/6 mice, 3 months old. We measured the effect of morphine with and without suvorexant on the pain threshold using an IITC PE34 Incremental Thermal Nociceptive Threshold Analgesia Meter (IITC Life Science Inc.), which raises the temperature of its aluminum surface at 6 °C min^{-1} in each trial. When the mouse licked or shook a hindlimb or jumped, the experimenter immediately pressed the stop switch and removed the

animal from the apparatus and recorded the surface temperature. Analgesia threshold was established on three consecutive days, with three tests per day, 15 min apart. The post drug tests were done starting 60 min after vehicle or morphine administration. Thirty six male mice (n = 6 per group) were used. Suvorexant (30 mg kg^{-1} in 0.5% methyl cellulose) or vehicle (0.5% methyl cellulose) was given orally 60 min before morphine (5 mg kg^{-1} or 10 mg kg^{-1}, SC). The animal was checked for any skin inflammation or lesion from the thermal test and would have been removed immediately from the experiment for treatment if either occurred, but this did not happen.

Statistical analyses

Data were subjected to ANOVA followed by Tukey post hoc test comparisons or t-test using the SYSTAT statistical package (SYSTAT). All such tests were two tailed. The results were considered statistically significant if $P < 0.05$. The number of subjects in each experimental procedure is indicated in the figure legends. All figures display standard error of the mean. All P values are two sided.

Reporting summary

Further information on research design is available in the Nature Portfolio Reporting Summary linked to this article.

Data availability

All data presented in this work have been deposited in G-Node (https://gin.g-node.org/fmfwu/Siegel_NatureMH_2024) and are available without restrictions from the corresponding author.

References

1. Cicero, T. J. No end in sight: the abuse of prescription narcotics. *Cerebrum* **2015**, 1–15 (2015).
2. Mack, K. A., Jones, C. M. & McClure, R. J. Physician dispensing of oxycodone and other commonly used opioids, 2000–2015, United States. *Pain Med.* **19**, 990–996 (2018).
3. Kelly, M. M., Reilly, E., Quinones, T., Desai, N. & Rosenheck, R. Long-acting intramuscular naltrexone for opioid use disorder: Utilization and association with multi-morbidity nationally in the Veterans Health Administration. *Drug Alcohol Depend.* **183**, 111–117 (2018).
4. Parthvi, R., Agrawal, A., Khanijo, S., Tsegaye, A. & Talwar, A. Acute opiate overdose: an update on management strategies in emergency department and critical care unit. *Am. J. Ther.* **26**, e380–e387 (2019).
5. Thannickal, T. C. et al. Human narcolepsy is linked to reduced number, size and synaptic bouton density in hypocretin-2 labeled neurons. *Abstr. Soc. Neurosci.* **26**, 2061 (2000).
6. Thannickal, T. C. et al. Reduced number of hypocretin neurons in human narcolepsy. *Neuron* **27**, 469–474 (2000).
7. Peyron, C. et al. A mutation in a case of early onset narcolepsy and a generalized absence of hypocretin peptides in human narcoleptic brains. *Nat. Med.* **6**, 991–997 (2000).
8. Thannickal, T. C. et al. Opiates increase the number of hypocretin-producing cells in mouse and human brain, and reverse cataplexy in a mouse model of narcolepsy. *Sci. Transl. Med.* **10**, eaao4953 (2018).
9. Fragale, J. E., James, M. H. & Aston-Jones, G. Intermittent self-administration of fentanyl induces a multifaceted addiction state associated with persistent changes in the orexin system. *Addict. Biol.* **26**, e12946 (2021).
10. James, M. H. et al. Increased number and activity of a lateral subpopulation of hypothalamic orexin/hypocretin neurons underlies the expression of an addicted state in rats. *Biol. Psychiatry* **85**, 925–935 (2019).
11. Guilleminault, C. & Cao, M. T. in *Principles and Practice of Sleep Medicine* (eds Kryger, M. H. et al.) 957–968 (Elsevier, 2011).
12. Darke, S., Kaye, S., Duflou, J. & Lappin, J. Completed suicide among methamphetamine users: a national study. *Suicide Life Threat. Behav.* **49**, 328–337 (2019).
13. Zhu, J., Spencer, T. J., Liu-Chen, L. Y., Biederman, J. & Bhide, P. G. Methylphenidate and μ opioid receptor interactions: a pharmacological target for prevention of stimulant abuse. *Neuropharmacology* **61**, 283–292 (2011).
14. Ponz, A. et al. Abnormal activity in reward brain circuits in human narcolepsy with cataplexy. *Ann. Neurol.* **67**, 190–200 (2010).
15. Schwartz, S. et al. Abnormal activity in hypothalamus and amygdala during humour processing in human narcolepsy with cataplexy. *Brain* **131**, 514–522 (2007).
16. Kiyashchenko, L. I. et al. Release of hypocretin (orexin) during waking and sleep states. *J. Neurosci.* **22**, 5282–5286 (2002).
17. McGregor, R., Wu, M.-F., Barber, G., Ramanathan, L. & Siegel, J. M. Highly specific role of hypocretin (orexin) neurons: differential activation as a function of diurnal phase, operant reinforcement vs. operant avoidance and light level. *J. Neurosci.* **31**, 15455–15467 (2011).
18. Mileykovskiy, B. Y., Kiyashchenko, L. I. & Siegel, J. M. Behavioral correlates of activity in identified hypocretin/orexin neurons. *Neuron* **46**, 787–798 (2005).
19. Wu, M. F., Nienhuis, R., Maidment, N., Lam, H. A. & Siegel, J. M. Role of the hypocretin (orexin) receptor 2 (Hcrt-r2) in the regulation of hypocretin level and cataplexy. *J. Neurosci.* **31**, 6305–6310 (2011).
20. Wu, M. F., Nienhuis, R., Maidment, N., Lam, H. A. & Siegel, J. M. Cerebrospinal fluid hypocretin (orexin) levels are elevated by play but are not raised by exercise and its associated heart rate, blood pressure, respiration or body temperature changes. *Arch. Ital. Biol.* **149**, 492–498 (2011).
21. Blouin, A. M. et al. Human hypocretin and melanin-concentrating hormone levels are linked to emotion and social interaction. *Nat. Commun.* **4**, 1547 (2013).
22. Farahimanesh, S., Zarrabian, S. & Haghparast, A. Role of orexin receptors in the ventral tegmental area on acquisition and expression of morphine-induced conditioned place preference in the rats. *Neuropeptides.* **66**, 45–51 (2017).
23. Meye, F. J., van Zessen, R., Smidt, M. P., Adan, R. A. H. & Ramakers, G. M. J. Morphine withdrawal enhances constitutive μ-opioid receptor activity in the ventral tegmental area. *J. Neurosci.* **32**, 16120–16128 (2012).
24. Stefano, G. B. & Kream, R. M. Endogenous morphine synthetic pathway preceded and gave rise to catecholamine synthesis in evolution (review). *Int. J. Mol. Med.* **20**, 837–841 (2007).
25. Baimel, C. et al. Orexin/hypocretin role in reward: implications for opioid and other addictions. *Br. J. Pharmacol.* **172**, 334–348 (2015).
26. Vittoz, N. M., Schmeichel, B. & Berridge, C. W. Hypocretin/orexin preferentially activates caudomedial ventral tegmental area dopamine neurons. *Eur. J. Neurosci.* **28**, 1629–1640 (2008).
27. Narita, M. et al. Direct involvement of orexinergic systems in the activation of the mesolimbic dopamine pathway and related behaviors induced by morphine. *J. Neurosci.* **26**, 398–405 (2006).
28. Balcita-Pedecino, J. J. & Sestak, S. R. Orexin axons in the rat ventral tegmental area synapse infrequently onto dopamine and gamma-aminobutyric acid neurons. *J. Comp. Neurol.* **503**, 668–684 (2007).
29. Ji, K., Miyauchi, J. & Tsirka, S. E. Microglia: an active player in the regulation of synaptic activity. *Neural Plast.* **2013**, 627325 (2013).
30. Schafer, D. P., Lehrman, E. K. & Stevens, B. The 'quad-partite' synapse: microglia–synapse interactions in the developing and mature CNS. *Glia* **61**, 24–36 (2013).

31. Zhan, Y. et al. Deficient neuron–microglia signaling results in impaired functional brain connectivity and social behavior. *Nat. Neurosci.* **17**, 400–406 (2014).

32. Taylor, A. M. W. et al. Neuroimmune regulation of GABAergic neurons within the ventral tegmental area during withdrawal from chronic morphine. *Neuropsychopharmacology* **41**, 949–959 (2016).

33. Vilca, S. J., Margetts, A. V., Pollock, T. A. & Tuesta, L. M. Transcriptional and epigenetic regulation of microglia in substance use disorders. *Mol. Cell. Neurosci.* **125**, 103838 (2023).

34. Hutchinson, M. R. et al. Reduction of opioid withdrawal and potentiation of acute opioid analgesia by systemic AV411 (ibudilast). *Brain Behav. Immun.* **23**, 240–250 (2009).

35. Hutchinson, M. R. et al. Minocycline suppresses morphine-induced respiratory depression, suppresses morphine-induced reward, and enhances systemic morphine-induced analgesia. *Brain Behav. Immun.* **22**, 1248–1256 (2008).

36. Maduna, T. et al. Microglia express mu opioid receptor: insights from transcriptomics and fluorescent reporter mice. *Front. Psychiatry* **9**, 726 (2019).

37. Xiong, X. et al. Mitigation of murine focal cerebral ischemia by the hypocretin/orexin system is associated with reduced inflammation. *Stroke* **44**, 764–770 (2013).

38. Vickers, A. P. Naltrexone and problems in pain management. *BMJ* **332**, 132–133 (2006).

39. Spitzer, N. C. Neurotransmitter switching? No surprise. *Neuron* **86**, 1131–1144 (2015).

40. Liu, B., Kwok, R. P. S. & Fernstrom, J. D. Colchicine-induced increases in immunoreactive neuropeptide levels in hypothalamus: use as an index of biosynthesis. *Life Sci.* **49**, 345–352 (1991).

41. McGregor, R. et al. Hypocretin/orexin interactions with norepinephrine contribute to the opiate withdrawal syndrome. *J. Neurosci.* **42**, 255–263 (2022).

42. Juarez-Portilla, C. et al. Brain activity during methamphetamine anticipation in a non-invasive self-administration paradigm in mice. *eNeuro* **5**, 1–14 (2018).

43. LeSauter, J., Balsam, P. D., Simpson, E. H. & Silver, R. Overexpression of striatal D2 receptors reduces motivation thereby decreasing food anticipatory activity. *Eur. J. Neurosci.* **51**, 71–81 (2020).

44. Spitzer, N. C. Activity-dependent neurotransmitter respecification. *Nat. Rev. Neurosci.* **13**, 94–106 (2012).

45. McGregor, R., Shan, L., Wu, M. F. & Siegel, J. M. Diurnal fluctuation in the number of hypocretin/orexin and histamine producing: implication for understanding and treating neuronal loss. *PLoS ONE* **12**, e0178573 (2017).

46. Georgescu, D. et al. Involvement of the lateral hypothalamic peptide orexin in morphine dependence and withdrawal. *J. Neurosci.* **23**, 3106–3111 (2003).

47. Ma, H. et al. Excitation–transcription coupling, neuronal gene expression and synaptic plasticity. *Nat. Rev. Neurosci.* **24**, 672–692 (2023).

48. Yap, E. L. & Greenberg, M. Activity-regulated transcription: bridging the gap between neural activity and behavior. *Neuron* **100**, 330–348 (2018).

49. Yamanaka, A., Tabuchi, S., Tsunematsu, T., Fukazawa, Y. & Tominaga, M. Orexin directly excites orexin neurons through orexin 2 receptor. *J. Neurosci.* **30**, 12642–12652 (2010).

50. Robinson, J. D. & McDonald, P. H. The orexin 1 receptor modulates kappa opioid receptor function via a JNK-dependent mechanism. *Cell. Signal.* **27**, 1449–1456 (2015).

51. Keith, D. R. et al. Time of day influences the voluntary intake and behavioral response to methamphetamine and food reward. *Pharmacol. Biochem. Behav.* **110**, 117–126 (2013).

52. Kosobud, A. E. K., Pecoraro, N. C., Rebec, G. V. & Timberlake, W. Circadian activity precedes daily methamphetamine injections in the rat. *Neurosci. Lett.* **250**, 99–102 (1998).

53. Paqueron, X. et al. Is morphine-induced sedation synonymous with analgesia during intravenous morphine titration? *Br. J. Anaesth.* **89**, 697–701 (2002).

54. Obukuro, K. et al. Nitric oxide mediates selective degeneration of hypothalamic orexin neurons through dysfunction of protein disulfide isomerase. *J. Neurosci.* **33**, 12557–12568 (2013).

55. John, J. et al. Greatly increased numbers of histamine cells in human narcolepsy with cataplexy. *Ann. Neurol.* **74**, 786–793 (2013).

56. Jalewa, J., Wong-Lin, K., McGinnity, T. M., Prasad, G. & Holscher, C. Increased number of orexin/hypocretin neurons with high and prolonged external stress-induced depression. *Behav. Brain Res.* **272**, 196–204 (2014).

57. Palomba, M. et al. Alterations of orexinergic and melanin-concentrating hormone neurons in experimental sleeping sickness. *Neuroscience* **290**, 185–195 (2015).

58. Crocker, A. et al. Concomitant loss of dynorphin, NARP, and orexin in narcolepsy. *Neurology* **65**, 1184–1188 (2005).

59. Lopresti, N. M., Esguerra, M. & Mermelstein, P. G. Sex differences in animal models of opioid reward. *Curr. Sex. Health Rep.* **12**, 186–194 (2020).

60. Ito, D. et al. Microglia-specific localisation of a novel calcium binding protein, Iba1. *Mol. Brain. Res.* **57**, 1–9 (1998).

61. Maldonado, R. et al. Reduction of morphine abstinence in mice with a mutation in the gene encoding CREB. *Science* **273**, 657 (1996).

Acknowledgements

Author contributions

R.M., M.-F.W., T.C.T. and J.M.S. designed the study. R.M. ran the anatomical experiments, M.-F.W. ran the behavioral experiments (wheel running and analgesia) and T.C.T. and S.L. ran the microglial studies. R.M., M.-F.W., T.C.T., S.L. and J.M.S. analyzed the results and R.M., M-F.W., T.C.T. and J.M.S. wrote the paper.

Competing interests

The authors declare no competing interests.

Additional information

Supplementary information The online version contains supplementary material available at https://doi.org/10.1038/s44220-024-00278-2.

Correspondence and requests for materials should be addressed to Jerome M. Siegel.

Peer review information *Nature Mental Health* thanks John Peever and the other, anonymous reviewer(s) for their contribution to the peer review of this work.

Reprints and permissions information is available at www.nature.com/reprints.